TRACKING BREAST CANCER TUMOR GROWTH AND ANGIOGENESIS WITH PERFLUOROCARBON MICROBUBBLES

by

Danny Robles

A Thesis Submitted to the Faculty of the

DEPARTMENT OF CELLULAR AND MOLECULAR MEDICINE

In Partial Fulfillment of the Requirements

For the Degree of

MASTER OF SCIENCE

In the Graduate College

THE UNIVERSITY OF ARIZONA

2016

STATEMENT BY AUTHOR

The thesis titled *Tracking Breast Cancer Growth and Angiogenesis with Perfluorocarbon Microbubbles* prepared by Danny Robles has been submitted in partial fulfillment of requirements for a master's degree at the University of Arizona and is deposited in the University Library to be made available to borrowers under rules of the Library.

Brief quotations from this thesis are allowable without special permission, provided that an accurate acknowledgement of the source is made. Requests for permission for extended quotation from or reproduction of this manuscript in whole or in part may be granted by the head of the major department or the Dean of the Graduate College when in his or her judgment the proposed use of the material is in the interests of scholarship. In all other instances, however, permission must be obtained from the author.

SIGNED: **Danny Robles**

APPROVAL BY THESIS DIRECTOR

This thesis has been approved on the date shown below:

Terry Matsunaga	**July 1st 2016**
Thesis Director Name	Date

Acknowledgements

I would like to thank the Experimental Mouse Shared Services Laboratory for their assistance with the handling and preparation of our mice models.

I also want to thank Dr. Russell Witte and Pier Ingram for their help with the Matlab analysis program and for teaching me how to use the Vevo ultrasound machine.

A special thanks to Dr. Terry Matsunaga for all of his support and mentorship over the last few years.

I want to acknowledge the Arizona Research Laboratories as well as the NIH for their financial support. (T.O.M. CA185684)

Table of Contents

Abstract

Objective: In this study, I have directly tracked the progression of angiogenesis for three different types of breast cancer cell lines; MDA-MB-231, MCF-7, and MDA-MB-468. Each of these cell lines is known to overexpress different receptors, which may affect a tumor's growth rate and perhaps its ability to undergo angiogenesis. Here, I measure and compare the growth, extent, and time of onset for angiogenesis.

Methods: I used SCID mice to profile each of the different breast cancer cell lines. The growth rate of each tumor, along with its blood vessel development, was monitored and imaged using lipid-coated microbubbles and contrast-enhanced ultrasound (CEUS). A Vevo 2100 pre-clinical ultrasound machine was used for the imaging experiments. To track development of angiogenesis, mice were injected with perfluorobutane gas microbubbles of 1-2 microns diameter. Bubble perfusion into the tumor is an indicator of the presence of blood vessel formation. A custom image analysis program was developed in Matlab™ to eliminate breathing artifacts and track microbubble motion based on their high temporal frequency signature ("flicker").

Results: My experiments demonstrated that, although different cell lines grow at different rates, microbubbles begin to penetrate the tumor when it reaches approximately a size of approximately 3 mm in diameter. Therefore, the onset of angiogenesis occurred at different times (MCF-7 occurring first at around 9 days, MDA-MB-468 occuring at 12 days post inoculation, and MDA-MB-231 occurring at 17 days post tumor cell inoculation). Matlab^{TM} analysis demonstrates consistent angiogenic behavior among the three cell lines.

Conclusion: For all cell lines, angiogenesis started when the volume of the tumor was approximately 21.76 mm^3, consistent with previous studies. As angiogenesis progressed, there was a drop in tumor blood flow. This can be explained by the sudden influx of oxygen when angiogenesis first begins. This momentarily inhibits new blood vessel formation while the tumor continues to steadily grow. After this sudden drop, tumor vascularization resumes a steady increase.

Introduction

Over the past 20 years, mortality rates due to breast cancer have been declining due to improved early detection methods and medical advances in treatment. Nevertheless, the incidence of breast cancer still ranks first among all other forms of cancer in women [1]. In 2012, breast cancer in the United States was responsible for one-third of all cancers diagnosed in women. Yet despite medical advances, breast cancer is still the second leading cause of cancer related death among women [1]. Understanding the behavior of malignant breast tumors, in particular their vascular development, can lead to better diagnostic and therapeutic treatments that may decrease these staggering numbers.

Breast cancer is an extremely complex disease and there can be significant variation between the cancer cells of one patient and another [2]. One of these differences involves the receptors that are overexpressed on the surface of breast cancer cells. Overexpression of specific receptors on the cell surfaces is considered a hallmark of cancer cells [3]. Cancer cells are capable of changing receptors they express in order to promote the transmission of pro-growth signals [3]. In breast cancer, the human epidermal growth factor receptor (EGFR) is the receptor most commonly overexpressed. Nearly 10% of breast carcinomas have EGFR gene amplification and protein overexpression according to a previous study [4]. In addition, estrogen and progesterone receptors are also commonly overexpressed in breast cancer resulting in the observation that the growth of breast cancer cells is often regulated by steroid hormones and peptide hormone receptors [5]. In turn, these overexpressed receptors have become potential targets for breast cancer therapy due to the ability to selectively target therapeutic agents to tumor cells over healthy normal cells. For example, human epidermal growth factor gene (HER-2) is currently being targeted to prevent cancer cells from progressing into a metastatic state [6]. Figure 1 offers a schematic comparing the receptors on a normal cell with those on a cancer cell. The excessive number of HER2 is a focus of current treatments that are exploiting this difference in receptor population. A third breast cancer phenotype is defined as one lacking the expression of estrogen and progesterone receptors along with no overexpression of the HER-2 gene [7]. These triple-negative breast cancer cells are known for being difficult to treat, as they have less biomarkers to target. Despite these differences, all of these tumors share a common trait; that being the size for the time of onset for angiogenesis [8,9].

Tumors require a constant supply of nutrients in order for them to continue rapid growth. A tumor's limit of nutrient diffusion occurs when it is between 1-2 mm in diameter [8,9]. For tumors to grow

past this limit, they must have an increased blood supply. The formation of new blood vessels, herein referred to as angiogenesis, is the mechanism by which a >2 mm tumor continues to receive the essential nutrients necessary for continued growth. The process of angiogenesis is initiated by cellular hypoxia, which allows hypoxic inducible factor-1 (HIF-1) protein to increase the synthesis of vascular endothelial growth factor (VEGF). VEGF, along with other pro-angiogenic factors, initiates new blood vessel formation in tumors. Angiogenesis may also be an indicator that a breast tumor is transitioning from a benign to a malignant state as new vessels increase the opportunity for cancer cells to undergo hematogenous spread via the circulation [10]. Therefore, being able to detect when new blood vessel formation begins could help lead to early detection of malignancy as well as possible therapeutic interventions. Unfortunately, no form of breast cancer behaves exactly the same as another. Forms may grow and proliferate, or become malignant at different rates. To explore these possibilities, I attempted to profile three different forms of breast cancer development using breast adenocarcinoma cells that expressed the most common receptors. In this study, we measure and compare the growth and angiogenesis rates of these different forms of breast cancer.

Microbubbles made from perfluorobutane gas with a lipid coating are stable at body temperature (37°C). They resonate in an ultrasound beam, rapidly contracting and expanding in response to pressure changes of the wave. In 2-dimensional B mode imaging, these contrast agents are capable of reflecting the sound wave echoes at the same wavelength as they were administered. These microbubbles thus show a very bright display in the 2-dimensional ultrasound image, making them easily detectable [11]. These gas microbubbles can travel through the vasculature and have a life span (~4 minutes) sufficient to interrogate new vascular development in a tumor environment [12,13]. They are able to travel through the vasculature while being tracked via contrast–enhanced ultrasound (CEUS), making them ideal for following the progression of tumor angiogenesis. In principle, as blood vessels in a tumor begin to form, the microbubbles will begin to perfuse through the tumor, making its angiogenic activity visible by clinical ultrasound.

Previous literature indicates that the initiation of blood vessel formation is only dependent on tumor size [8,9]. Therefore, I predict that all three different breast cancer cell lines being studied will begin angiogenesis at approximately similar tumor sizes. However, because of the different receptors being

expressed on the cancer cells, the timing of each tumor reaching that size may differ. Excessive EGFR mediated intracellular signaling has been shown to contribute to the transformation of cellular phenotypes and provide tumor cells with substantial growth and survival advantages [14]. Similarly, estrogen receptors overexpressed on breast cancer cells are responsible for excessive mitogenic signaling, which controls cellular proliferation and differentiation [15]. As such, it is possible that the cell lines that overexpress growth factor receptors (MCF-7s and MDA-MB-231s) will grow faster than the cells that lack receptor overexpression (MDA-MB-468). There are no previous studies that suggest the progression of vessel formation will differ in these different breast tumors. Therefore, the progression of angiogenesis in all of these different tumors will follow a similar behavior if the null hypothesis is correct. After the onset of angiogenesis, it is predicted that the rate of blood vessel formation will continue to increase linearly as the tumor continues to grow.

Methods

Microbubble preparation

Microbubbles were made by mixing 10 mol % 1,2-Distearoyl-sn-Glycero-3-Phosphoethanolamine-N-[Maleimide(Polyethylene Glycol)2000] (Ammonium Salt)(DPPE PEG2000), 82 mol % 1,2-Dipalmitoyl-sn-glycero-3-phosphocoline (DPPC), 8 mol % 1,2-Dipalmitoyl-sn-glycerol-3-phosphate (Monosodium Salt)(DPPA). These lipids were then dispersed in a solvent comprising 80% saline, 15% propylene glycol, and 5% glycerol by volume (1 mg/mL). Approximately 1.5 mL of the mixture was placed in a vial. The vials were capped and purged with perfluorobutane gas for 30-45 seconds. The purged vials were then placed in a modified dental amalgamator (Vialmix^{TM}) for 45 seconds at 4000 RPM to create the microbubbles. On the day of the experiments, the bubbles were further diluted to a 1:3 suspension with 0.85% (w/v) saline prior to intravenous injection.

Mice Models

Female SCID mice were anesthetized with isoflurane and the ventral side of the left hind leg was shaved and surgically cleaned. In lieu of tail-vein injections, femoral catheters were placed for microbubble injection. An incision ~ ½ cm long was made over the top of the femoral vein and artery. The vein was isolated with 6-0 silk suture, a small cut made, and a mouse femoral vein catheter (SAI Infusion Technologies) was advanced into the vein and tied in. The catheter was then tunneled subcutaneously to the back of the head and tied in. Wound clips were used to close both wounds and the animal was allowed to recover. Breast cancer cells (MDA-MB-231, MCF-7, and MDA-MB-468) were grown in culture for several days until they were about 80% confluent. The cell count was then approximated using a hemocytometer. Approximately 5 X 10^5 cells were injected subcutaneously into the mammary fat pad. MCF-7 cells were additionally injected with an estrogen pellet of 0.25 mg with a 21 day release. The mice were ready to be imaged 2 days after inoculation of cells.

Cell lines: MDA-MB-231 cells overexpress EGFR on their surface. MCF-7s have estrogen receptors overexpressed on their surface, and MDA-MB-468s are triple negative breast cancer cells, lacking the expression of estrogen and progesterone receptors along with no overexpressed EGFR.

Contrast Enhanced Ultrasound Imaging

Mice models inoculated with one of three different breast cancer cell lines, were imaged beginning two days after implanting tumor cells. The mice were anesthetized by being individually placed in a chamber and induced with 4% isoflurane gas followed by 1.5-2% maintenance. The mouse was then placed on the

platform of the Visualsonics VEVO 2100 pre-clinical ultrasound machine. A 40 MHz transducer was used to image these animals and the VEVO machine was set to 5% power with a frame rate of 10-25 frames per second (fps) and a dynamic range of 70 db. The area of interest on the mouse was covered with ultrasound gel and the transducer lowered until the tumor was clearly seen on the VEVO screen. A series of 2-dimensional images 0.05 mm apart spanning the length of the entire tumor were taken for 3-dimensional reconstruction on post-image processing. This was used to estimate the tumor volume. Doppler mode was also used to determine directional blood flow as well as to potentially view new blood vessel formation via inward and outward movement. Doppler flow was also used to observe and compare changes with time. Finally, B-mode (2-dimensional imaging) was used to view the tumor before and after the injection of approximately 150 μL of gas-filled microbubbles. A total of two injections per animal were recorded for each experiment. Mice were imaged twice weekly beginning two days post-inoculation. Once the microbubbles were seen to clearly penetrate the tumor, the mouse was imaged two additional times for confirmation and for further analysis of vascular development. After mice demonstrated microbubble penetration for a total of three consecutive experiments, they were sacrificed and the tumor excised for histology.

Quantifying Microbubble Activity with MATLAB® Data Processing

In B-mode, motion artifacts such as the flow of microbubbles produce ”flicker” from frame to frame. As such, with the help of a collaborating lab, a Matlab program was created in order to isolate and quantitate bubble density inside the tumor. The Matlab code allowed for the suppression of low frequency components such as breathing artifacts and peristaltic bowel movement on the ultrasound movie. Suppressing these elements as dark background would allow the fast moving, high frequency microbubbles to be highlighted in green. For each experiment with the VEVO pre-clinical ultrasound machine, the largest tumor cross –sectional areas were displayed in B-mode and it was that “slice” that was analyzed for microbubble penetration with the Matlab™ software.

Results

Table 1:

Cell Line	Number of Mice Used	Average Time to Microubble Perfusion (Days)	Range for microbubble perfusion (Days)	Average Tumor Volume at time of microbubble perfusion (mm^3)	Range of Volume (mm^3)
MDA-MB-468 (Triple Negative)	**7**	**12.1 +/- 2.6**	**9 - 16**	**17.4 +/- 6.2**	**6.5 – 25.4**
MDA-MB-231 (EGFR overexpression)	**9**	**17 +/- 7.0**	**7 - 27**	**23.3 +/- 6.9**	**10 – 30.9**
MCF-7 (Estrogen receptor overexpression)	**8**	**9.4 +/- 2.0**	**7 - 14**	**24.6 +/- 6.9**	**16.5 – 34**

Table 1 provides data of the three cell lines used for this study including; 1) time of microbubble perfusion in days; and 2) volume of the tumors in mm^3. Microbubble perfusion inside the tumor was used as an indicator for blood vessel formation. The data indicates that among all three different cell lines, there is no significant difference in what the size of the tumor is when angiogenesis begins. Across all cell lines, the average size of the tumor when microbubble perfusion is first observed is 21.76 +/- 3.8 mm^3. Assuming a spherical structure, microbubble perfusion begins when the tumor diameter is 3.46 mm on average. This is a larger diameter than what Folkman had previously claimed to be 1-2 mm. One aspect of the data that does vary between all three-breast cancer cell lines is the time it takes to see microbubble perfusion in these tumors. This may be due to the fact that these cell lines are growing at different rates as shown in Figure 2. MCF-7s, for example, show the most rapid growth compared to the other two cell lines. If the start of angiogenesis (as indicated by CEUS) depends only on tumor size, then it would be expected that MCF-7 cells would begin blood vessel formation earlier than the other two cell lines. This was confirmed by the data in Table 1.

MCF-7

The MCF-7 cell line, which is estrogen and progesterone receptor positive, clearly showed the fastest growth rate. Figure 2 shows that this cell line grows nearly twice as fast as the MDA-MB468s and the MDA-MB 231s. However, when inoculating mice with this cell line it is standard to promote growth via implanting an estrogen pellet. This estrogen is probably the reason why MCF-7 cells are observed to grow

so much faster. Regardless of the growth rate, microbubble perfusion consistently began when the tumor was approximately 24.6 +/- 6.9 mm^3 in volume at an average of 9.4 +/- 2 days after inoculation of the cancer cells.

Assessment of Angiogenic Vessel Density: Using a code written in Matlab™, videos obtained using the VEVO ultrasound machine were processed to eliminate breathing and motion artifacts. Once these artifacts were removed, the code allowed for the measurement of intensity changes over a specified area throughout the image. Figure 3 shows a series of experiments performed on one mouse that was injected with the MCF-7 breast cancer cell line. The images depict the tumor development 2, 9, 11, 16, and 18 days after initial inoculation. The green color on the images indicates intensity changes (movement) recorded over time. Initially, there is no green inside the tumor, which is outlined in red. This lack of "flicker" inside the tumor indicates that blood vessels have not yet formed two days post inoculation. This is expected, as the cross-sectional area of the tumor is only 1.95 mm^2 at this time. Nine days post-inoculation, microbubble perfusion was observed and in Figure 3, the movement and intensity changes (flicker) that result because of the bubble perfusion are captured and highlighted in green. The image now shows the "flicker", an indication that microbubbles have penetrated the tumor demonstrating that the process of angiogenesis is occuring. At this point, the cross-sectional area of the tumor is considerably larger at 4.14 mm^2 and it has exceeded the tumor's limit of nutrient diffusion. The next recorded experiment again showed microbubbles perfusing the tumor but this time, interestingly, the recorded tumor blood flow relative to the tumor area decreased. The following two data acquisitions showed a steady increase in tumor blood flow. This behavior was consistent among all of the MCF-7 mice models. The Matlab™ software allowed us to obtain percentage values for the tumor blood flow relative to the cross-sectional area of the tumor for every experiment. A graph plotting the average tumor blood flow percentage vs. time in days after breast cancer cell inoculation is shown in Figure 5. Average tumor growth vs. time using the cross-sectional area of the tumors is also shown in Figure 6. On average, the cross-sectional area of MCF-7 tumors increased by 0.3 mm^2 per day and displayed a linear relationship with an R^2 value of 0.924.

MDA-MB-231

The MDA-MB-231 cell line, which overexpressed EGFR, displayed the most inconsistent behavior among all three cell lines studied. On average, their growth rate was slower than the MCF-7s and slightly faster than the MDA-MB-468s. However, the standard deviation for the growth rate was too high to conclude that this was significant. The average volume of the tumor when blood vessel perfusion was first observed was 23.3 +/- 6.9 mm^3. This volume is similar to the volume when angiogenesis was first seen on MCF-7 cells (24.6 mm^3 vs. 23.3 mm^3).

Assessment of Angiogenic Vessel Density: Blood flow in these tumors showed very similar behavior to the MCF-7 cell line. An initial increase in vasculature nine days after inoculation was seen followed by a sudden decrease in day 12. On average, the tumor blood flow as a function of tumor area decreased by 5% during this drop. This was again followed by an increase in tumor blood flow as shown in Figure 7. The growth of the tumor, by cross-sectional area, is shown in Figure 8. The cross sectional area in these tumors is increasing in a linear fashion.

MDA-MB-468

The MDA-MB-468 cells, which are triple negative, appeared to grow at approximately the same rate as the MDA-MB-231 cell. On average, microbubbles were observed to penetrate the tumor when it reached a volume of 17.4 +/- 6.2 mm^3. This was a slightly smaller volume than what was observed for the other two cell lines but still within one standard deviation, meaning this small difference was insignificant.

Assessment of Angiogenic Vessel Density: Tumor blood flow in this cell line appeared to be much less than the other two cell lines. In Figure 9, we can see that the highest percentage of blood flow per tumor area is only 20%. However, it follows a very similar behavior to the other two cell lines; there is a peak at day 16 followed by a sudden drop leading up to day 20. Prior to day 16, there appears to be a smaller peak between days 5-10. The percentage of tumor blood flow is only 10% and this does not consistently correlate with when the "flicker" created by the bubbles first appeared in these experiments. That small peak could be a result of not having a large enough sample size. This apparent bimodal distribution could be a result of outlier mice that showed bubble perfusion sooner than the majority. Figure 10 shows that the cross-sectional area of this cell line is increasing in a linear manner

Figures

Figure 1

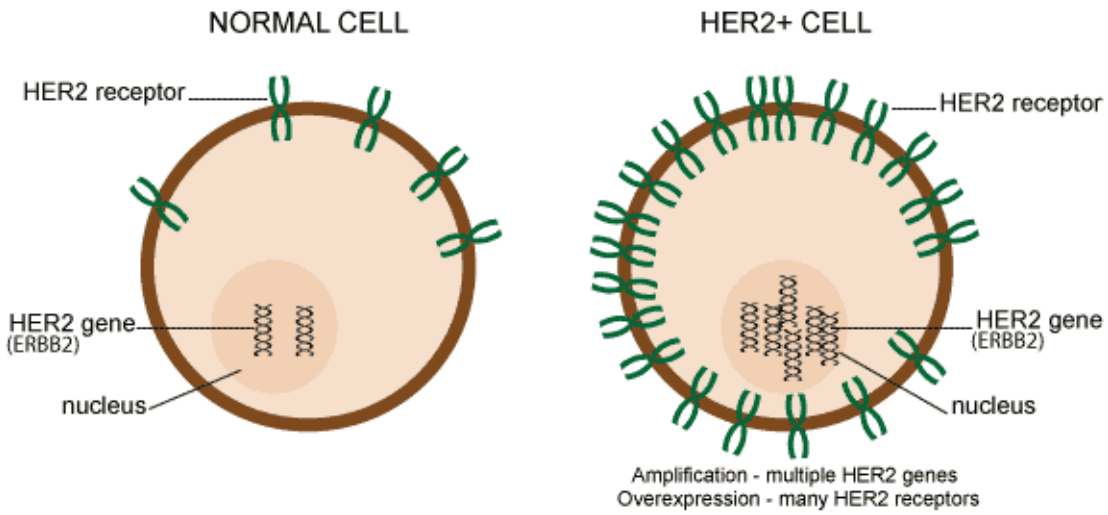

Figure 1. Increase in number of human epidermal growth factor receptors on the surface of cancer cells. Normally, one cell will express an estimated 20,000 of these receptors. Cancer cells however, will express as many as 2 million of these receptors on their surface, highly promoting receptor activation which leads to increased signaling, excessive cellular division, and tumor formation [15]. This principle applies when describing the overexpression of different receptors such as estrogen and progesterone.

Figure 2

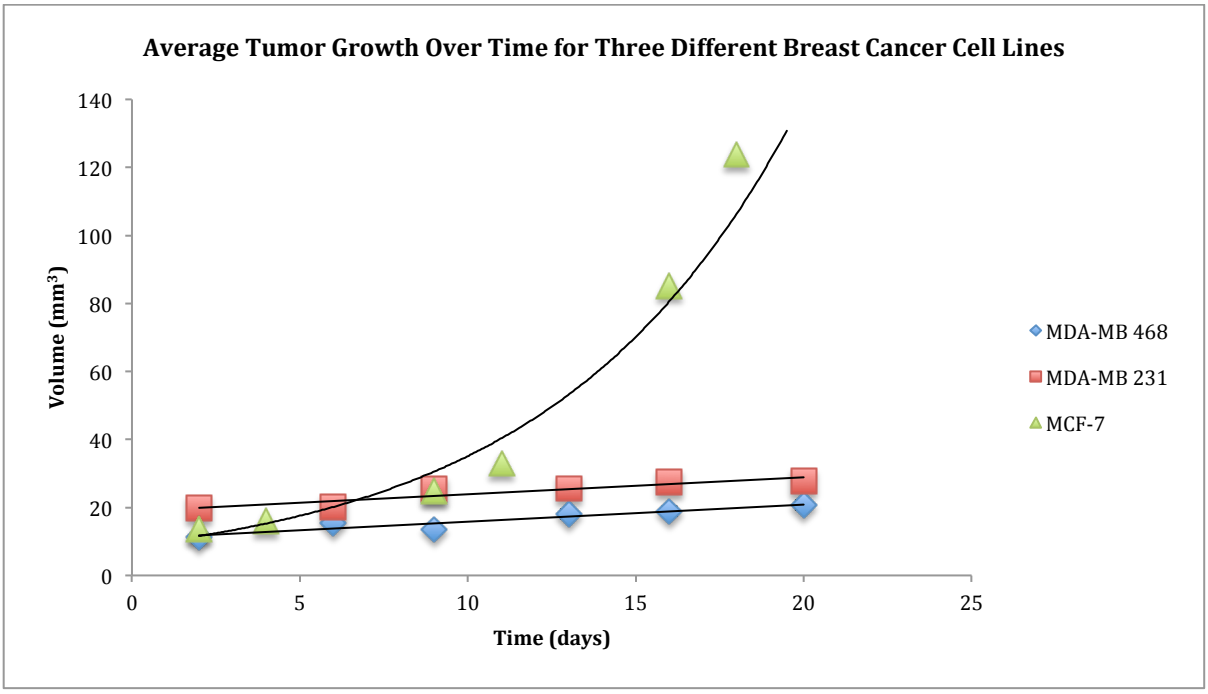

Figure 2. Average tumor growth for three different breast cancer cell lines as a function of the number of days after inoculation. It is clear that MCF-7s proliferate much faster than the other two cell lines. There is no significant difference between the growth rates of the MDA-MB-231 and the MDA-MB-468 cell lines. Based on this data, it is expected that MCF-7 cells will begin angiogenesis before the other two cell lines. However, because of the estrogen pellet that is also added upon cell inoculation, it is not likely that the rate of growth for MCF-7s is much faster than the others.

Figure 3

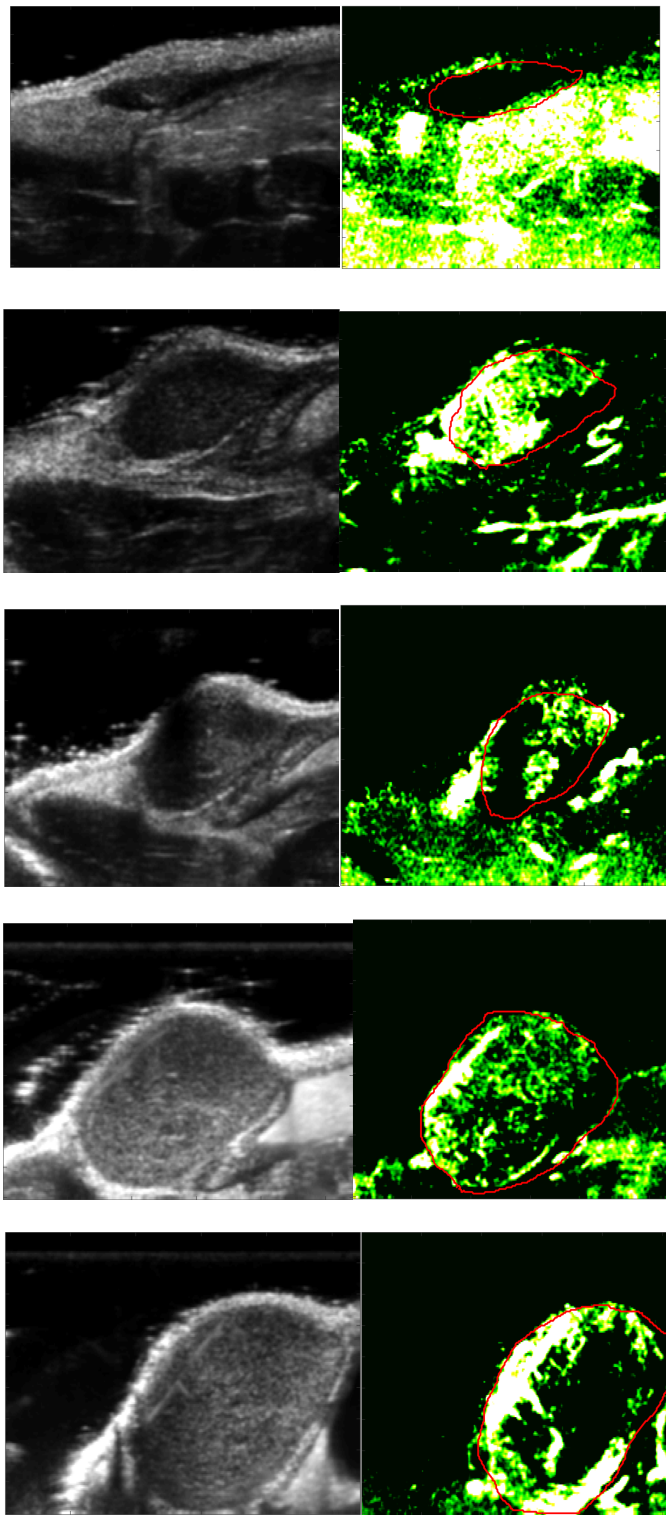

Day: 2
Area: 1.95 mm^2
perBubroi: 7.87%

Day: 9
Area: 4.14 mm^2
perBubroi: 56.81 %

Day: 11
Area: 3.38 mm^2
perBubroi: 28.0%

Day: 16
Area: 7.82 mm^2
perBubroi: 25.59%

Day: 18
Area: 8.80 mm^2
perBubroi: 37.98%

Figure 3. Extracted frames from the ultrasound B-mode movie immediately following microbubble injection. On the right, the images have the tumor area outlined in red and the green corresponds to the intensity changes caused by the fast moving microbubbles. Green inside the tumors indicates angiogenic

vessel development in tumors. For every set of images, the number of days after cancer cell inoculation at which they were taken is given, along with the area of the outlined tumor region. The Matlab program also gave a percentage value for the amount of high intensity shown inside the outlined tumor area, labeled here as perBubroi. A higher percentage value corresponds to more vasculature inside the tumor. The images show that 4 days post-inoculation, there are almost no intensity changes seen inside the tumor. At day 9, there is a huge jump in perBubroi, indicating that angiogenesis has started. This data was obtained for all of the experiments that were performed.

Figure 4

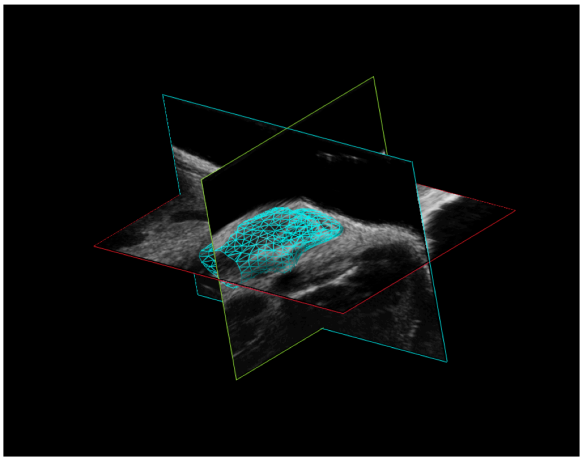

Figure 4. VEVO 2100 software generated 3D reconstruction of an MDA-MB 468 tumor approximately 20 days after inoculation. Tumor volumes are automatically calculated once the reconstruction is completed.

Figure 5

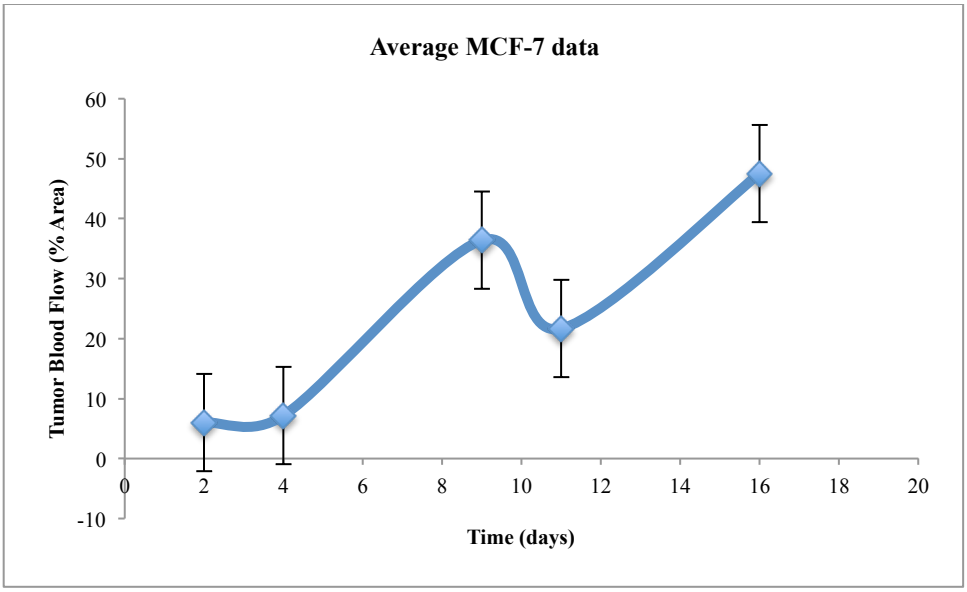

Figure 5. Average percent tumor blood flow vs. time in days since inoculation with MCF-7 breast cancer cells. The data for the tumor blood flow was collected using developed Matlab™ software. The figure is significant for an increase in tumor blood flow between days 4 and 9 post-inoculation. The sharp increase in tumor blood flow indicates new blood vessel formation. Following this sharp increase, there is a sudden drop in the percent of tumor blood flow relative to the tumor area, between days 9-11. This is followed by a steady increase in blood flow after day 11.

Figure 6

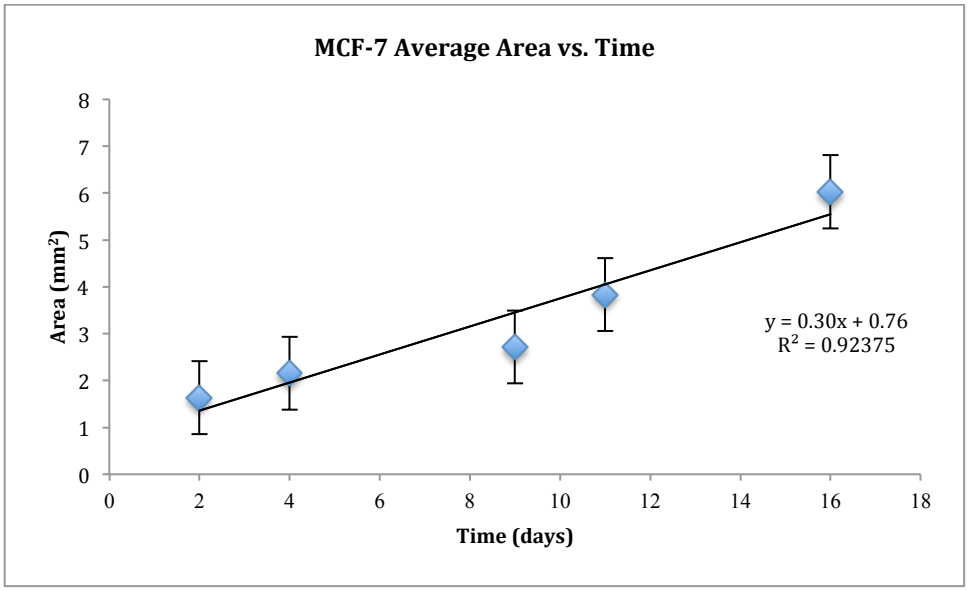

Figures 6. Average tumor cross-sectional area vs. time in days after injection. There appears to be a linear correlation in regards to tumor growth over time. The analyzed data indicates that the largest cross-sectional area of MCF-7 tumors is increasing, on average, by approximately 0.30 mm^2 per day. The data was calculated to have an R^2 value of 0.923, indicating a linear correlation between tumor cross-sectional area growth and time.

Figure 7

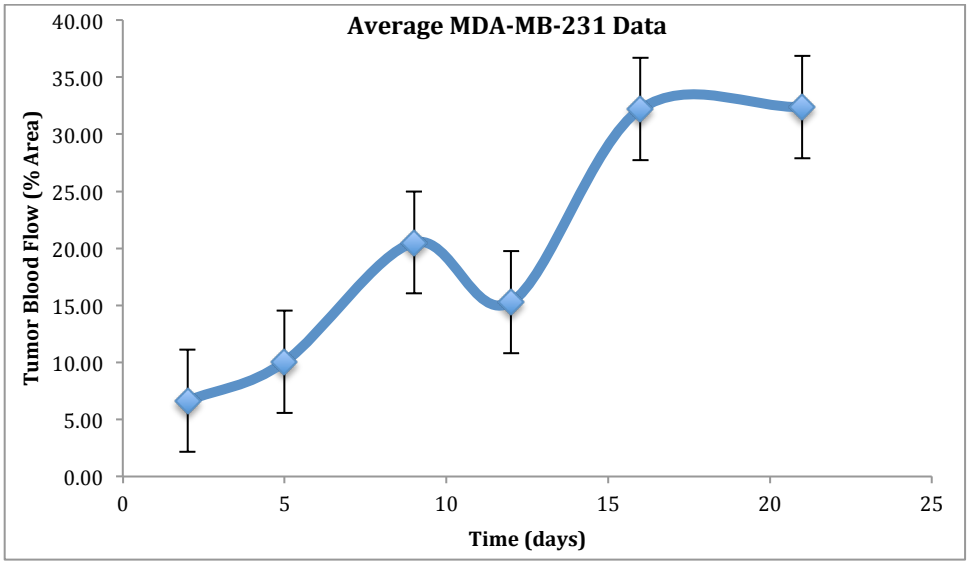

Figure 7. Average percentage of tumor blood flow vs. time in days for five mice inoculated with MDA-MB-231 breast cancer cells. The figure shows a sharp increase in tumor blood flow between days 5 and 9. The sharp increase in tumor blood flow indicates new blood vessel formation. A sudden drop at day 11 followed by a steady increase in tumor blood flow up to day 16.

Figure 8

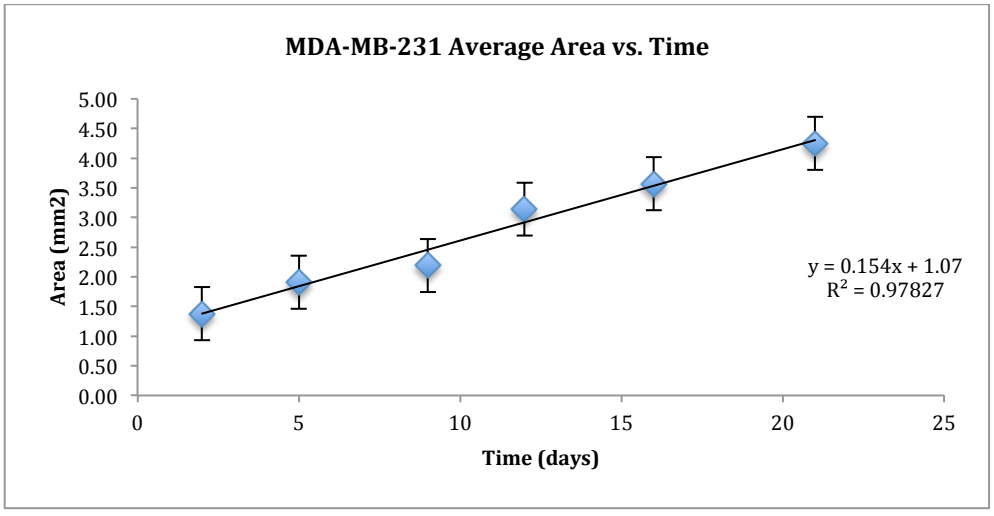

Figures 8. Average tumor cross-sectional area vs. time in days after injection with MDA-MB-231 cells. This data was collected using the Matlab software. There is a linear correlation in regards to tumor growth over time. The graph indicates that the cross-sectional area of MDA-MB 231 tumors is increasing, on

average, by approximately 0.15 mm^2 per day (R^2 value=0.978, indicating a linear correlation between tumor cross-sectional area growth and time).

Figure 9

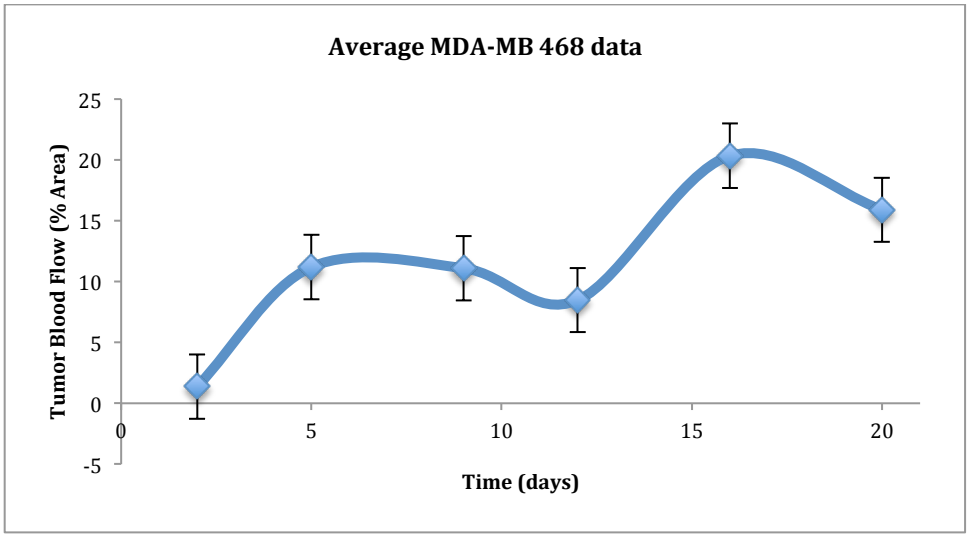

Figure 9. Average percentage of tumor blood flow vs. time in days for five mice inoculated with MDA-MB-468 breast cancer cells. The figure initially shows an increase in tumor blood flow at day 5 with a minor dip before day 12. During this time period, the highest percent for tumor blood flow does not exceed 12%. This makes it unlikely that the intensity changes recorded were due to microbubbles. At day 12, there is a large increase in tumor blood flow peaking at day 16. After that, a sudden decline is seen on the graph leading up to day 20.

Figure 10

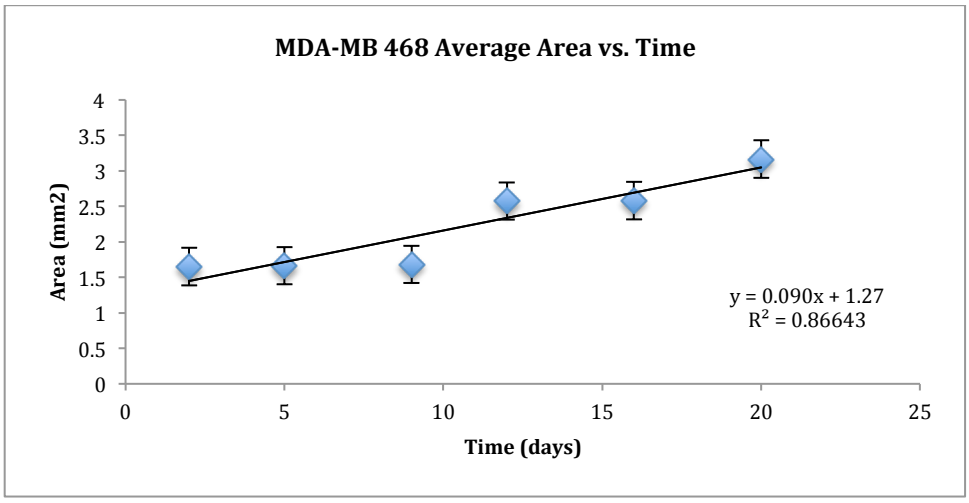

Figures 10. Average tumor cross-sectional area vs. time in days after injection with MDA-MB-468 cells. The data was fitted for a linear curve and an R^2 value of 0.866 shows that there is a linear correlation between cross-sectional area and time. The graph indicates that the cross-sectional area of MDA-MB 468 tumors is increasing, on average, by approximately 0.09 mm^2 per day.

Discussion

The aim of this project was to profile the angiogenic as well as proliferative behaviors of three of the most common forms of breast adenocarcinomas; MCF-7s, MDA-MB 231s, and MDA-MB 468s using lipid-coated microbubbles and CEUS. Using a SCID mouse model, we were able to implement this non-invasive technique and qualitatively determine the time of onset for angiogenesis in the breast cancer cell lines by looking at microbubble perfusion inside the tumors. Furthermore, using the Vevo LAB software, we were able to calculate the exact volume of the tumors throughout all of the experiments. This allowed for the comparison of the size of the tumors upon the onset of angiogenesis as well as the tracking of the growth rate for each tumor over time. Among the three different breast cancer cell lines used in this study, there was no significant difference in the volume of the tumor when angiogenesis was first observed. The average volume for the start of angiogenesis among all 24 mice used in the study was 21.76 +/- 3.8 mm^3. Assuming a spherical structure, microbubbles were able to perfuse inside the newly formed vasculature in the tumor when it reached a diameter of approximately 3.46 mm. While this is slightly above the limit of nutrient diffusion as predicted by Folkman and others, this may be due to the infrequency of our observation or the irregular shapes of the actual tumors [8,9]. Tumors do not grow in a spherical manner. The 3-dimensional images of the tumors show that they are far from spherical and this could be a reason why the approximated diameter was slightly larger than the standard. Furthermore, tumors were analyzed bi-weekly, meaning there were several days in between experiments. Depending on the growth rate of the tumor, it is highly likely that angiogenesis may have begun on a non-experimental day, which could have slightly skewed the calculated volume for the onset of angiogenesis to a higher number than it should have been. Nevertheless, these experiments showed that tumor size is the only determinant for the initiation of angiogenesis. The overexpression of different receptors on the breast cancer cells seemed to have no effect on the onset of angiogenesis. The data indicated that reaching the limit of nutrient diffusion, which leads to cellular hypoxia, is what begins the process of angiogenesis.

The growth rate of the three different tumors varied according to the data collected. In a clinical setting, breast tumors vary tremendously in terms of their aggressiveness. Those that overexpress extracellular receptors may grow at a faster rate because the increased intracellular signaling provides for

increased cell growth and survival [14,15]. Therefore, I predicted a similar behavior would be observed in our own *in vivo* experiments. The estrogen and progesterone receptor positive cells (MCF-7s) had a growth rate significantly higher than the other two cell lines. Seven days after the inoculation of the cancer cells in the mice, the tumor size began to linearly increase with its volume shown to increase by an average of 9.33 mm^3 per day. By comparison, the MDA-MB 231 and the MDA-MB 468 cell lines steadily increased in volume by 0.50 mm^3 and 0.47 mm^3, respectively, starting at two days post inoculation. This difference in growth rates leads to a variation in the time of onset for angiogenesis. Not surprisingly, mice inoculated with MCF-7 cells showed new blood vessel formation the earliest, as they reached the critical volume much earlier than MDA-MB 231 and MDA-MB 468 tumor models. Again, it is important to note that MCF-7 mice models were injected with an estrogen pellet and this could explain why this cell line was growing much faster than the others. Unfortunately, there is no way to inoculate mice with MCF-7 cells without also adding the estrogen pellet to induce growth and therefore, we cannot make the claim that this cell line has the fastest growth rate. Nevertheless, the perfusion of microbubbles inside the tumor was observed, on average, 9 days post inoculation for the MCF-7 cell line, just over 12 days post inoculation for the MDA-MB 468 cell line, and 17 days post inoculation for the MDA-MB 231 cell line. MDA-MB-468 and MDA-MB-231s were not shown to significantly differ from each other in terms of growth rate. These results do not support the idea that the increased cell signaling resulting from the overexpressed receptors may have an observed impact on the growth rate of tumors only. The start of angiogenesis, among the 3 different tumor models studied, was conserved and shown to be dependent on tumor size alone.

The progression of angiogenesis in all three different tumor models showed similar behaviors. Using the Matlab™ software, we were first able to confirm that what we classified as microbubbles on the live B-mode ultrasound movies were indeed microbubbles. The “flicker”, non-existent prior to microbubble injection, was a result of the microbubbles reflecting the sound waves being generated from the ultrasound transducer. Furthermore, using the “flicker” we were able to track the progression of this vascular development by looking at the percentage of bubbles inside the tumor as a function of the cross sectional area of these tumors. Analyzing this data would give us a better understanding of the rate of vascular development in comparison with the growth rate of the tumors. As expected, the results showed a sharp increase in tumor blood flow right at the onset of angiogenesis. But to our surprise, this was followed by a

sharp decline in tumor blood flow several days later. After this unexpected decline, tumor blood flow seemed to steadily increase. To our knowledge, this is the first study on angiogenesis that has tracked and quantified the formation of blood vessels in this manner. A mechanism that we propose for the obtained results is the following; Focusing on the molecular initiation of vascular formation, angiogenesis begins when pro-angiogenic factors such as the vascular endothelial growth factor (VEGF) are being synthesized at high levels. This happens when cells are under hypoxic stress and the process is mediated by the hypoxic inducible factor 1 protein (HIF-1). Under normoxia, the product of the Von Hippel-lindau (VHL) gene, a tumor suppressor, binds to the HIF1 protein and degrades it to prevent the transcription of pro-angiogenic factors [16]. When a tumor reaches its limit of nutrient diffusion, it is undergoing hypoxic stress. With such minimal amount of oxygen entering the cells, HIF-1s become stabilized and are no longer hydroxylated. This prevents VHL from binding and degrading HIF-1 [16]. HIF-1s are thus allowed to contribute to carcinogenesis by stimulating the expression of vascular endothelial growth factor as well as a number of other genes that drive angiogenesis and metastasis. When new vasculature is formed inside the tumor, there will be a huge influx of oxygen that will be delivered to the "starving" cells. This influx of oxygen will lead to hydroxylation of the HIF-1 protein and it would thus be tagged for degradation by VHL. Without HIF-1, there is no synthesis of VEGF meaning no angiogenesis. Consistent with our current results, it is possible that after the initial formation of new vasculature, the sudden influx of oxygen momentarily inhibits angiogenesis. The tumor however, continues to steadily increase in size. If this is true, it could potentially explain the behavior of angiogenic progression that was observed from the Matlab™ analysis. As seen in the figures, when angiogenesis begins, there is a huge spike in vessel formation followed by a drop a few days later due to the momentary inhibition of angiogenesis and the continued growth of the tumor. As the tumor continues to grow, it once again becomes hypoxic and vessel formation progressively follows.

As previously mentioned, this proposed mechanism is just one possibility for the obtained results. Because this behavior was consistent among nearly all of the mice studied, the confidence on the results is high. There are however, several factors that need to be considered. First, it is important to note that we are only analyzing one slice of the three dimensional tumor. In each experiment, we look at the slice with the largest tumor cross-sectional area, but it is possible that we are not observing exactly the same slice in

every experiment. This would also imply that the rate of growth inside the tumor is not uniform which indeed is a possibility. In fact, it is doubtful that the rate of angiogenesis is uniform from one section to the next. This could potentially impact the percentage of vessel formation recorded on different experimental days. There may have also been an error when outlining the tumor area in the Matlab software. If the periphery of the tumor was outlined, it could give us a false indication of vessel formation. This can become an even bigger problem if there is substantial movement of the mouse during the image processing. Movement of the mouse could shift the outlined tumor area towards the tumor periphery or even further out. This potential phenomenon was taken into consideration when outlining the tumors and closely monitored when analyzing the data. By playing the videos that were being analyzed, we were able to confirm that what we outlined as tumor at the start of the video remained the area of interest throughout. If this was not the case, the area of interest was adjusted.

This study demonstrated the potential of gas-filled microbubbles as contrast agents for monitoring angiogenesis. Their ability to track the start and the progression of angiogenesis means they may have the potential to be used as a diagnostic as well as therapeutic tool. Here, we were able to profile three different forms of breast cancer cells. First, we showed that the initiation of angiogenesis for the three cell lines depends on the size of the tumors. This study further supported previous research by Folkman and others, who predicted that angiogenesis would begin when a tumor is between 1-2 mm in diameter. We were also able to track the growth rate of the three different tumors, and though it appeared that the cell lines that overexpressed receptors grew at a faster rate, the difference was not statistically significant to make that claim. Finally, we were able to track the progression of angiogenesis, something that has never been done using microbubbles and CEUS. The progression of new vascular development in the tumors showed an unexpected behavior; a sharp increase in tumor blood flow per percent area after the tumor reached its limit of nutrient diffusion followed by a sudden drop. The proposed mechanism that explains this observed behavior clearly needs to be further studied, perhaps by using markers against HIF-1 or VEGF and monitoring their expression levels. Nevertheless, we were able to show progressive behaviors of angiogenesis that have not been previously reported. Developing a better understanding for this process can lead to more effective therapeutic targets that will aid in the fight against breast cancer.

References

1. DeSantis, C., Siegel, R., Bandi, P., & Jemal, A. (2011). Breast cancer statistics, 2011. *CA: a cancer journal for clinicians*, *61*(6), 408-418.

2. Rosen, L. S., Ashurst, H. L., & Chap, L. (2010). Targeting signal transduction pathways in metastatic breast cancer: a comprehensive review. *The oncologist*, *15*(3), 216-235.

3. Hanahan, D., & Weinberg, R. A. (2000). The hallmarks of cancer. *cell*,*100*(1), 57-70.

4. Bhargava, R., Gerald, W. L., Li, A. R., Pan, Q., Lal, P., Ladanyi, M., & Chen, B. (2005). EGFR gene amplification in breast cancer: correlation with epidermal growth factor receptor mRNA and protein expression and HER-2 status and absence of EGFR-activating mutations. *Modern pathology*, *18*(8), 1027-1033.

5. Pietras, R. J., Arboleda, J., Reese, D. M., Wongvipat, N., Pegram, M. D., Ramos, L., ... & Slamon, D. J. (1995). HER-2 tyrosine kinase pathway targets estrogen receptor and promotes hormone-independent growth in human breast cancer cells. *Oncogene*, *10*(12), 2435-2446.

6. Ross, J. S., Slodkowska, E. A., Symmans, W. F., Pusztai, L., Ravdin, P. M., & Hortobagyi, G. N. (2009). The HER-2 receptor and breast cancer: ten years of targeted anti–HER-2 therapy and personalized medicine. *The oncologist*, *14*(4), 320-368.

7. Dawood, S. (2010). Triple-negative breast cancer. *Drugs*, *70*(17), 2247-2258.

8. Schneider, B. P., & Miller, K. D. (2005). Angiogenesis of breast cancer. *Journal of Clinical Oncology*, *23*(8), 1782-1790.

9. *Folkman J: Tumor angiogenesis: therapeutic implications. N Engl J Med**285**:1182-1186, 1971*

10. Weidner, N., Semple, J. P., Welch, W. R., & Folkman, J. (1991). Tumor angiogenesis and metastasis—correlation in invasive breast carcinoma. *New England Journal of Medicine*, *324*(1), 1-8.

11. Blomley, M. J., Cooke, J. C., Unger, E. C., Monaghan, M. J., & Cosgrove, D. O. (2001). Microbubble contrast agents: a new era in ultrasound. *British Medical Journal*, *322*(7296), 1222.

12. Unger, E. C., Porter, T., Culp, W., Labell, R., Matsunaga, T., & Zutshi, R. (2004). Therapeutic applications of lipid-coated microbubbles. *Advanced drug delivery reviews*, *56*(9), 1291-1314.

13. Sheeran, P. S., Luois, S. H., Mullin, L. B., Matsunaga, T. O., & Dayton, P. A. (2012). Design of ultrasonically-activatable nanoparticles using low boiling point perfluorocarbons. *Biomaterials*, *33*(11), 3262-3269.

14. Nicholson, R. I., Gee, J. M. W., & Harper, M. E. (2001). EGFR and cancer prognosis. *European journal of cancer*, *37*, 9-15.

15 Renoir, J. M., Marsaud, V., & Lazennec, G. (2013). Estrogen receptor signaling as a target for novel breast cancer therapeutics. *Biochemical pharmacology*, *85*(4), 449-465.

16 Maxwell, P. H., Wiesener, M. S., Chang, G. W., Clifford, S. C., Vaux, E. C., Cockman, M. E., ... & Ratcliffe, P. J. (1999). The tumour suppressor protein VHL targets hypoxia-inducible factors for oxygen-dependent proteolysis.*Nature*, *399*(6733), 271-275.